

DRAFT

THERMAL-MECHANICAL ANALYSIS OF PRESSURE VESSELS

Michael Benson, David Rudland, and Mark Kirk
US Nuclear Regulatory Commission
Rockville, MD, USA

The views expressed in this paper are those of the authors and do not reflect the views of the U.S. Nuclear Regulatory Commission.

ABSTRACT

Regulatory Guide (RG) 1.161 and American Society of Mechanical Engineers Boiler and Pressure Vessel Code (ASME Code), Section XI, Non-Mandatory Appendix K contain stress intensity factor (SIF) equations for both the internal pressure and thermal gradient loading cases. However, the technical basis behind these equations was developed only for $R_i/t = 10$, where R_i is the inner vessel radius and t is the vessel thickness. While this geometry is appropriate for most pressurized water reactors (PWR), most boiling water reactor (BWR) vessels have $R_i/t = 20$. This paper explores the validity of applying these SIF equations to BWRs. This confirmatory work includes calculating SIF by independent methods. The one-dimensional heat equation is solved to provide a physical basis for the thermal stresses.

NOMENCLATURE

RG	Regulatory Guide
ASME Code	American Society of Mechanical Engineers Boiler and Pressure Vessel Code
SIF	Stress Intensity Factor
PWR	Pressurized Water Reactor
BWR	Boiling Water Reactor
USE	Upper Shelf Energy
$K_{I_p}^{Axial}$	SIF Due to Internal Pressure for an Axial Flaw
SF	Safety Factor
p_a	Maximum Accumulation Pressure
R_i	Vessel Inner Radius
t	Vessel Wall Thickness
a	Crack Depth
F_i	Geometry Factors
K_{II}	SIF Due to Thermal Gradient
CR	Cooling Rate

r	Radial Position along Vessel Wall Relative to Cylinder Axis
c_p	Heat Capacity at Constant Pressure
T	Temperature
τ	Time
ρ	Density
k	Thermal Conductivity
q	Heat Flux
h_c	Convective Heat Transfer Coefficient
T_f	Fluid Temperature
T_s	Temperature at Vessel Inner Surface
R_o	Outer Radius
T_o	Initial Fluid Temperature
$\sigma_{\theta\theta}$	Hoop Stress
p	Internal Pressure
α	Coefficient of Thermal Expansion
E	Elastic Modulus
ν	Poisson's Ratio
σ_i	Polynomial Fitting Coefficients
x	Radial Position along Vessel Wall Relative to Inner Surface
G_i	Influence Coefficients for SIF Calculation
Q	Flaw Shape Parameter
c	Half the Crack Length
ϕ	Angular Position along Crack Front

INTRODUCTION

RG 1.161 and ASME Code XI Non-mandatory Appendix K provide a procedure for determining adequate upper shelf energy (USE), as determined from Charpy impact experiments, to protect against ductile fracture of nuclear reactor pressure vessels at operating temperature [1][2]. A necessary step toward determining the applied J-integral in this procedure is calculating the SIF due to internal pressure and thermal gradient loading, K_{I_p} and K_{II} , respectively. The equations used to calculate

DRAFT

B/24

DRAFT

SIF were developed from curve fitting of finite element results [3][4]. The finite element models, however, used $R_i/t = 10$, which is correct only for a PWR vessel geometry.

This paper explores the validity of applying the SIF equations to BWR vessel geometries. SIF was calculated by two independent methods: American Petroleum Institute (API) standard 579-1 and the method employed by the Fracture Analysis of Vessels-Oak Ridge (FAVOR) computer code [5][7]. The applied stresses were calculated using continuum mechanics principles. The thermal gradients for a 0.02 K/s (100 R/hr) cooldown transient were determined by solving the one-dimensional heat equation. While the RG/Appendix K methods discuss equations for both axial and circumferential cracks, this work considered only the equations for axial cracks, since these equations were found to give the highest SIF.

RG 1.161/APPENDIX K SIF EQUATIONS

The RG 1.161 equation for calculating SIF due to internal pressure, $K_{I_p}^{Axial}$ [ksi-in.^{0.5}], is shown in Equations 1 and 2.

$$K_{I_p}^{Axial} = (SF) p_a [1 + (R_i/t)] (\pi a)^{0.5} F_1 \quad (1)$$

$$F_1 = 0.982 + 1.006(a/t)^2 \quad (2)$$

where SF is the safety factor, p_a [ksi] is the maximum accumulation pressure, a [in.] is the crack depth, and F_1 is a geometry factor. Equation 1 is valid for $0.05 \leq a/t \leq 0.50$. The SIF due to thermal gradient is calculated according to Equations 3 and 4.

$$K_{II} = [(CR)/1000]^{2.5} F_3 \quad (3)$$

$$F_3 = 0.69 + 3.217(a/t) - 7.435(a/t)^2 + 3.532(a/t)^3 \quad (4)$$

where CR is the cooling rate and F_3 is a geometry factor. Equation 3 is valid for $0.2 \leq a/t \leq 0.50$ and $0 \leq CR \leq 100^\circ\text{F/hr}$. The units for Equations 1 and 3 must be in the Customary system.

CALCULATION OF THERMAL GRADIENTS

The cooldown transient is simulated by solving the one-dimensional heat equation in cylindrical coordinates (Equation 5).

$$\rho c_p \frac{\partial T}{\partial \tau} = \frac{1}{r} \frac{\partial}{\partial r} \left(k r \frac{\partial T}{\partial r} \right) \quad (5)$$

where ρ is the density of the vessel steel, c_p is the specific heat of the vessel steel, T is the temperature at a particular radial position and time, τ is the time, r is the radial position, and k is the thermal conductivity of the vessel steel.

The boundary conditions at the inside and outside surfaces of the vessel are shown in Equations 6 and 7, respectively.

$$q = h_c (T_f - T_s) \text{ for } r = R_i \text{ and all } \tau \quad (6)$$

$$q = 0 \text{ for } r = R_o \text{ and all } \tau \quad (7)$$

where q is the heat flux, h_c is the convective heat transfer coefficient, T_f is the fluid temperature, T_s is the inside surface temperature of the vessel, and $R_o = R_i + t$. T_f is determined by Equation 8.

$$T_f = T_0 - (CR)\tau \quad (8)$$

where T_0 is the initial fluid temperature. The coolant temperature was allowed to decrease to 294 K and subsequently held constant. T_s was estimated at each time step by the numerical method employed to solve Equation 5.

The initial condition for this problem is stated in Equation 9.

$$T = T_0 \text{ for all } r \text{ and } \tau = 0 \quad (9)$$

Equation 5 is a parabolic partial differential equation, and various methods exist to solve it with the given boundary and initial conditions [8]. For example, Reference [3] employed finite element analysis. This work used a commercial software package that employs the discretization method described in [9] to numerically solve Equation 5.

CALCULATION OF STRESSES

The through-wall hoop stress profiles for pressure and thermal loading were calculated using well-known continuum mechanics equations. The hoop stress, $\sigma_{\theta\theta}$, for a thick-walled pressure vessel under internal pressure, p , is shown in Equation 10 [6].

DRAFT

DRAFT

$$\sigma_{\theta\theta} = \frac{pR_i^2}{R_o^2 - R_i^2} \left[1 + \left(\frac{R_o}{r} \right)^2 \right] \quad (10)$$

The hoop stress due to a thermal gradient in a cylinder is given by Equation 11 [3], [10].

$$\sigma_{\theta\theta} = \frac{\alpha E}{1-\nu} \frac{1}{r^2} \left(\frac{r^2 + R_i^2}{R_o^2 - R_i^2} \int_{R_i}^{R_o} T r dr + \int_{R_i}^r T r dr - T r^2 \right) \quad (11)$$

where α is the thermal expansion coefficient of the vessel, E is the elastic modulus of the vessel, and ν is Poisson's ratio of the vessel.

Calculation of SIF

Three independent methods were employed in this work to calculate SIF. The API 579-1 method uses a 4th order polynomial fit to the through-wall stress profile, as in Equation 12 [5][6].

$$\sigma(x) = \sigma_0 + \sigma_1 \left(\frac{x}{t} \right) + \sigma_2 \left(\frac{x}{t} \right)^2 + \sigma_3 \left(\frac{x}{t} \right)^3 + \sigma_4 \left(\frac{x}{t} \right)^4 \quad (12)$$

where x is the position from the inner radius, σ is the stress at position x , and σ_i are fitting coefficients. The mode I SIF, K_I , is then calculated with Equation 13.

$$K_I = \left[\sigma_0 G_0 + \sigma_1 G_1 \left(\frac{a}{t} \right) + \sigma_2 G_2 \left(\frac{a}{t} \right)^2 \right] \sqrt{\frac{\pi a}{Q}} + \dots \quad (13)$$

$$\left[\sigma_3 G_3 \left(\frac{a}{t} \right)^3 + \sigma_4 G_4 \left(\frac{a}{t} \right)^4 \right] \sqrt{\frac{\pi a}{Q}}$$

where G_i are tabulated influence coefficients determined by finite element analysis and Q is the flaw shape parameter (Equations 14 and 15).

$$Q = 1 + 1.464 \left(\frac{a}{c} \right)^{1.65} \quad \text{for } a/c \leq 1.0 \quad (14)$$

$$Q = 1 + 1.464 \left(\frac{c}{a} \right)^{1.65} \quad \text{for } a/c > 1.0 \quad (15)$$

where c is half the crack length.

The FAVOR method is similar in concept to the API 579-1 method. The differences in the two methods include: (1) the through-wall stress profile is fit only up to the crack tip in the FAVOR method, while the entire through-wall profile is fit for the API 579-1 method; (2) a 3rd order polynomial is fit to the stress profile for the FAVOR method, as opposed to the 4th order polynomial for the API 579-1 method; and (3) the influence coefficients are different for the two methods.

The final method of calculating SIF is to use Newman and Raju [4] for the internal pressure case. Equation 1 is based upon their method, which is shown as Equation 16.

$$K_I = \frac{pR_i}{t} \sqrt{\pi \frac{a}{Q}} F \left(\frac{a}{c}, \frac{a}{t}, \frac{R}{t}, \phi \right) \quad (16)$$

where ϕ is the angular position along the crack front ($\phi = \pi/2$ for this work) and the form of the geometry factor, F , is given in [4].

Results

The inputs for the above analysis are tabulated in Table 1. Figure 1(a) shows a contour plot of $T(r, \tau)$, the solution to Equation 5, for all τ with time on the ordinate and radial position normalized to wall thickness on the abscissa. The most severe temperature gradient was observed between 15 000 and 20 000 s, so that region is shown in Figure 1(b). At around 15 000 s, the temperature decreased from ~420 K at $r = R_o$ to ~380 K at $r = R_i$. By 30 000 s, steady state was established.

The resulting hoop stress distribution is shown in Figure 2. A tensile stress develops at $r = R_i$, leading to compression at $r = R_o$. The highest stresses were observed between 5 000 and 20 000 s, after which the stresses tended toward 0. The SIF calculated according to the API 579-1 method for $a/t = 0.25$ is shown as a function of time in Figure 3. The SIF increases to a maximum value of 10 MPa-m^{0.5} at 14 000 s, then decreases relatively rapidly to 0. The thermal SIF computed at 14 000 s according to two methods are shown along with the RG/ASME Code equation for several crack depths in Figure 4. The three methods show reasonable agreement, with the RG/ASME Code method giving slightly higher SIF when $a/t \leq 0.4$.

For the internal pressure loading case, the hoop stress profile is shown in Figure 5. The hoop stress decreases linearly from ~400 MPa at $r = R_i$ to ~380 MPa at $r = R_o$. The resulting SIF calculated according to several

DRAFT

methods is shown in Figure 6 for a range of crack depths. Overall, the four methods show reasonable agreement. The RG/ASME Code method is overly conservative for $a/t > 0.5$, consistent with the limits placed upon the equation (i.e., $0 \leq a/t \leq 0.5$).

DISCUSSION

Thermal stresses arise from temperature gradients through the wall thickness. As the inside surface cools and contracts, it is constrained by the hotter material at the outer surface. The resulting stress distribution is tension at the inner surface and compression at the outer surface. As the temperature gradient grows more severe, so do the stresses. Therefore, Figure 3 is a good indicator of the severity of the temperature gradient.

Figure 4 shows that the thermal SIF decreases with increasing crack depth. Figure 3 shows that a compressive stress has developed by 0.6 through the wall thickness. Therefore, the decreasing SIF is a result of the influence of the compressive stress at the outer surface. Figures 4 and 6 demonstrate that the RG 1.161/ASME Code method bounds or agrees with the other methods considered here for a range of crack depths.

Figure 7 shows the effect of vessel thickness, with $R/t = 20$, on the thermal SIF. As the vessel increases in thickness, more severe temperature gradients develop. The maximum SIF during to the cooldown, therefore, increases with increasing vessel thickness. Equation 3 has an exponent of 2.5 on the vessel thickness term. Figure 7 shows that Equation 3 becomes increasingly conservative for BWR vessels as vessel thickness increases.

CONCLUSIONS

Overall, this work demonstrated that Equations 1 and 3 are appropriate for use in BWR vessels. Less severe temperature gradients are expected in BWR vessels, since they are generally thinner than PWR vessels. The R/t relationship in the internal pressure SIF equation adequately captured the effect of geometry when considering the two vessel types.

ACKNOWLEDGMENTS

The authors wish to acknowledge Drs. Matthew Kerr and Aladar Csontos at the U.S. Nuclear Regulatory Commission for their support of this work.

REFERENCES

- [1] Regulatory Guide 1.161, "Evaluation of Reactor Pressure Vessels with Charpy Upper Shelf Energy Less Than 50 ft-lb," U.S. Nuclear Regulatory Commission, 1995.
- [2] ASME Boiler & Pressure Vessel Code Section XI, "Rules for Inservice Inspection of Nuclear Power Plant Components," The American Society of Mechanical Engineers, 2010.
- [3] Welding Research Council Bulletin 413, "Development of Criteria for Assessment of Reactor Vessels with Low Upper Shelf Fracture Toughness," July 1996.
- [4] J. C. Newman, Jr. and I. S. Raju, J. Press. Vess. Tech., "Stress-Intensity Factors for Internal Surface Cracks in Cylindrical Pressure Vessels," 102, 1980, pp. 342-346.
- [5] API 579-1/ASME FFS-1, "Fitness-for-Service," 2007, pp. C1-C202.
- [6] T. L. Anderson, "Fracture Mechanics: Fundamentals and Applications," 3rd Edition, CRC Press, New York, pp. 385-449.
- [7] P. T. Williams, T. L. Dickson, and S. Yin, "Fracture Analysis of Vessels – Oak Ridge FAVOR, v09.1, Computer Code: Theory and Implementation of Algorithms, Methods, and Correlations," ORNL/TM-2010/5, 2009.
- [8] E. Kreyszig, "Advanced Engineering Mathematics," 9th Edition, John Wiley & Sons, Inc., Hoboken, pp. 535-598, 886-932.
- [9] R. D. Skeel and M. Berzins, "A Method for the Spatial Discretization of Parabolic Equations in One Space Variable," SIAM J. Sci. and Stat. Comput., Vol. 11, 1990, pp. 1-32.
- [10] S. P. Timoshenko and J. N. Goodier, "Theory of Elasticity," 3rd Edition, McGraw-Hill, New York, 1970.

DRAFT

DRAFT

Table 1: Input parameters for the thermal-mechanical analysis.

Description	Value
Geometry	
t	0.16 m [0.51 ft]
R_i/t	20.5
a/t	0.1 to 0.8
a/c	1/3
Material Properties	
E	2.0×10^5 MPa [4.2×10^6 kip/ft ²]
ν	0.30
α	1.30×10^{-5} m/m/K [7.20×10^{-6} ft/ft/R]
k	38 W/(m-K) [22 BTU/(hr-ft-R)]
ρ	7770 kg/m ³ [485 lb _m /ft. ³]
c_p	536 J/(kg-K) [0.13 BTU/(lb _m -R)]
Thermal Loading Conditions	
h_c	5673 W/(m ² -K) [1000 BTU/(hr-ft ² -R)]
CR	0.02 K/s [100 R/hr]
T_0	561 K [1010 R]
Mechanical Loading Conditions	
p	19.0 MPa [396 kip/ft ²]

DRAFT

DRAFT

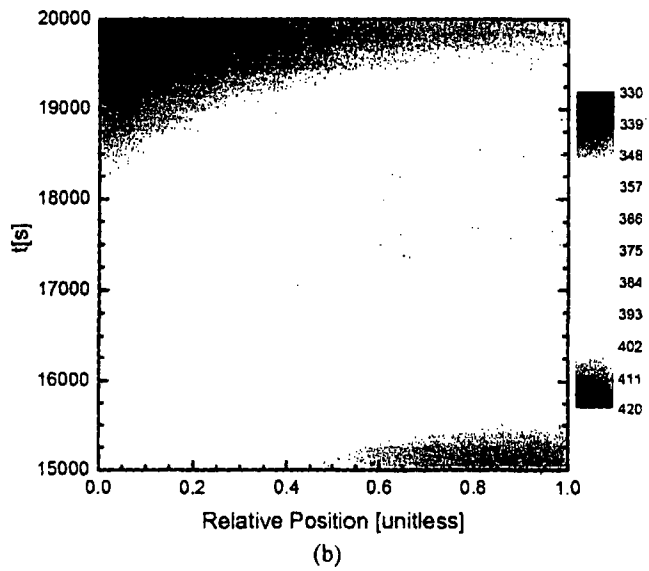
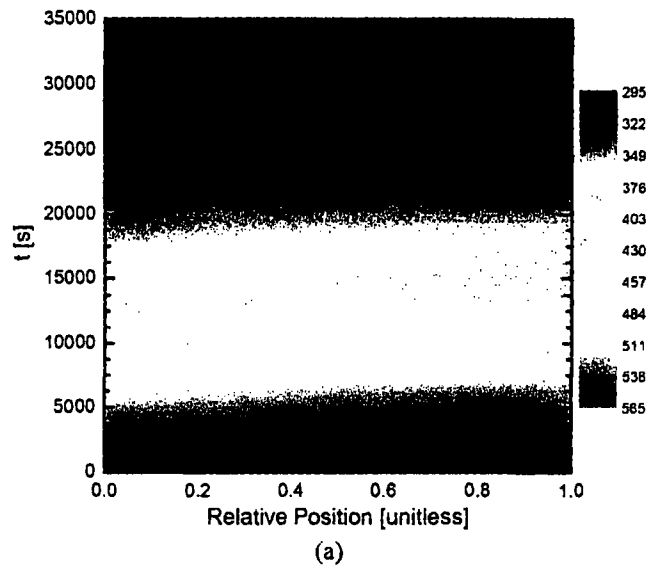


Figure 1: Temperature [K] contour plot for a 0.02 K/s cooldown transient in a BWR vessel: (a) entire transient and (b) between 15 000 and 20 000 s.

DRAFT

DRAFT

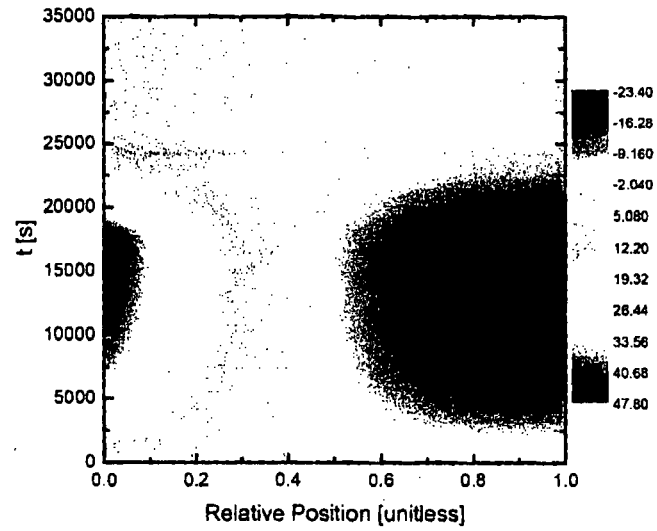


Figure 2: Stress distribution [MPa] during a 0.02 K/s cooldown transient for a BWR vessel.

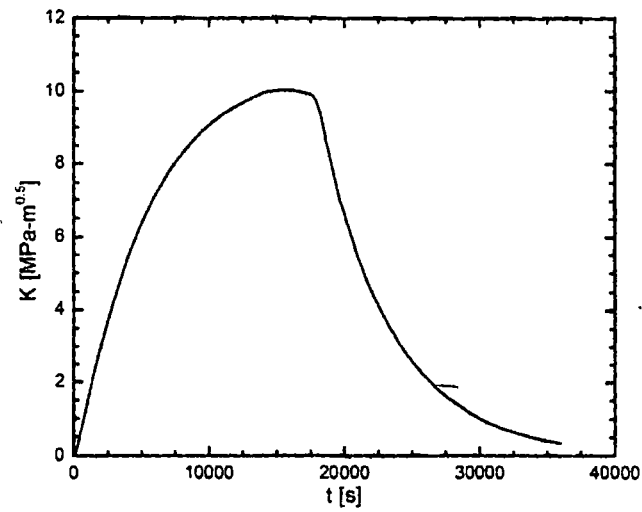


Figure 3: SIF against time for a 0.02 K/s cooldown transient in a BWR vessel.

DRAFT

DRAFT

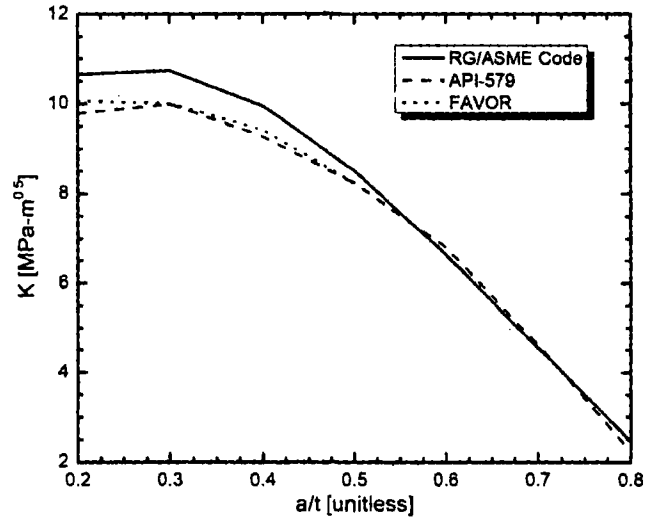


Figure 4: Comparison of three methods to calculate the SIF due to thermal gradients.

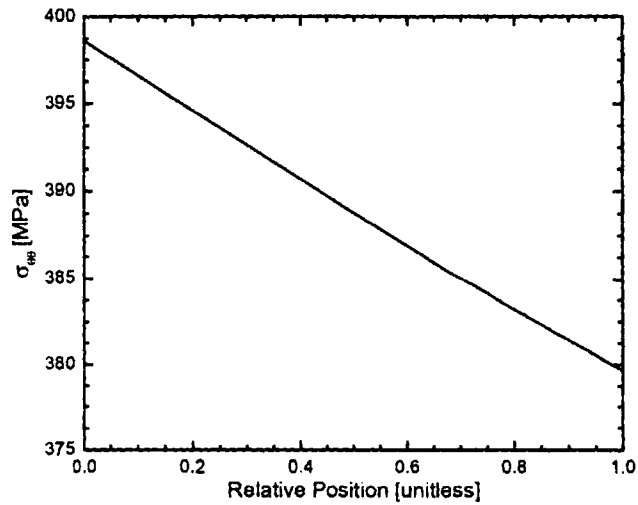


Figure 5: Hoop stress profile due to internal pressure in a BWR vessel.

DRAFT

DRAFT

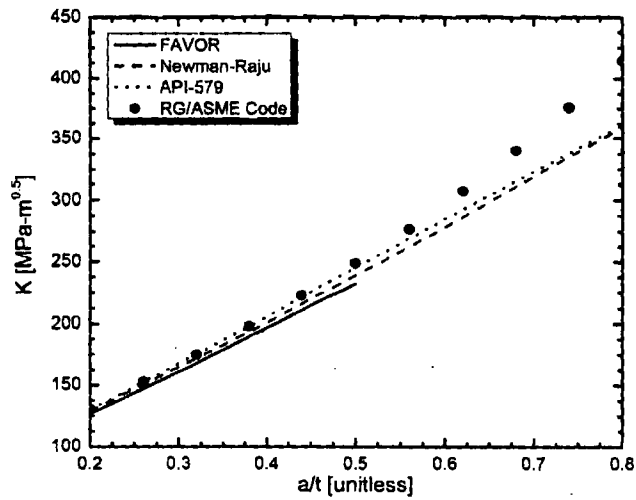


Figure 6: SIF, calculated according to several methods, due to internal pressure in a BWR vessel.

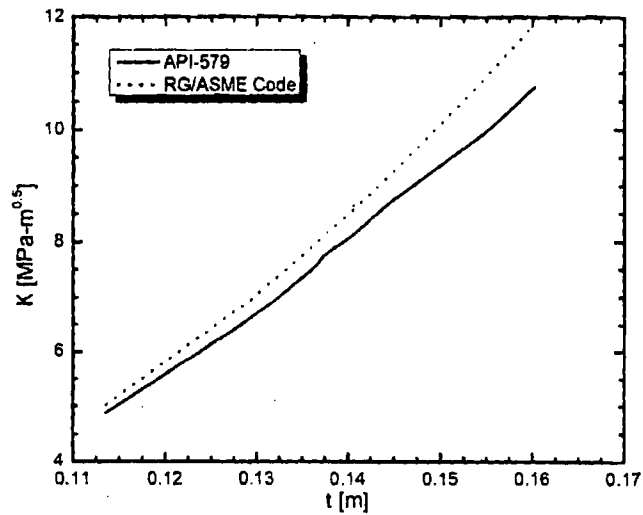


Figure 7: The effect of vessel thickness on SIF during a 0.02 K/s cooldown in BWR vessels.

DRAFT